Melting of monolayer plasma crystals

A. V. Ivlev, U. Konopka, and G. Morfill
Centre for Interdisciplinary Plasma Science, Max-Planck-Institut für Extraterrestrische Physik, D-85740 Garching, Germany

G. Joyce
Plasma Physics Division, Naval Research Laboratory, Washington, D.C. 20375-5346, USA
(Received 2 December 2002; published 18 August 2003)

Melting of a monolayer plasma crystal in a radio-frequency discharge with no particles suspended above or below is studied. The experimental data are compared with results of molecular dynamics simulations and theory. It is shown that the melting is caused by the resonance coupling between the longitudinal and the transverse dust-lattice wave modes, due to the interaction of particles with the plasma wakes.

DOI: 10.1103/PhysRevE.68.026405 PACS number(s): 52.27.Lw, 52.25.Gj, 52.35.−g

Most of the laboratory experiments on the investigation of plasma crystals are performed in a radio-frequency (rf) discharge [1–5]. Negatively charged microparticles are levitated in the sheath at the lower electrode, where the electrostatic force due to the vertical electric field is strong enough to compensate for gravity. Usually, particles form two-dimensional (2D) crystalline structures with one or a few horizontal particle layers. The crystals are shaped like a disc, suspended above the center of the electrode, and confined by a weak radial electric field.

There have been many papers on experimental [6–9] and theoretical [10,11] investigations of the formation and the melting of plasma crystals consisting of a few particle layers. The crystal-gas(liquid) transitions are believed to be induced by the ion current in the sheath: The melting is caused by the instability due to the asymmetric interaction between the particles and the plasma ''wakes'' [10] (the wakes are formed underneath the particles due to focusing of ions flowing to the electrode [12,13]). The crystallization occurs when the ion-dust two-stream instability becomes suppressed [11]. For bilayer crystals, the role of single ''dislocations'' (particles trapped above or below the crystal) as heat sources has been discussed [14]. However, there have been no experiments on the melting of monolayer crystals.

In this paper, we report on experimental study of melting of a *pure* monolayer with *no particles* suspended above or below. We compare the experiment with the results of molecular dynamics simulations and a previously proposed theory [15] and show that the melting is caused by the presence of wakes: The instability is induced by the resonance coupling between longitudinal and transverse dust-lattice (DL) wave modes, due to the particle-wake interaction.

Experiment. We used a rf plasma vessel that is based on the gaseous-electronics-conference (GEC) reference cell [16]. The original GEC-cell electrode geometry was changed for our experiments—the discharge was ignited between a lower rf-driven electrode of 100 mm diameter and an upper grounded electrode of 130 mm diameter (separated by 30 mm). A detailed description of the experimental setup is given in Ref. [17]. The chamber was filled with Ar gas, the pressure range was $p=1.5$–10 Pa. The rf peak-to-peak voltage was $\simeq 141$ V. After the plasma was ignited, monodisperse melamine-formaldehyde particles of 8.9 μm diameter and mass $\simeq 5.5\times 10^{-10}$ g were injected from above and confined over the center of the electrode. The horizontal confinement was provided by a weak radial electric field due to a copper ring with a height of 2 mm and an inner diameter of 40 mm placed on the electrode. The particles were illuminated by a horizontal laser sheet and recorded by a video camera from the top. The laser could be moved in the vertical direction together with the camera to observe the whole volume above the lower electrode.

In the beginning of each experiment, only a single particle or a pair of particles were injected. By following the particle trajectories—either the horizontal oscillations of a single particle or collisions between the two particles, we calculated (with the method proposed by Konopka *et al.* [17]) the radial profile of the horizontal confinement, the particle charge Q, and the screening length λ of the pair interaction (Yukawa) potential. In this paper, we consider an experiment performed at pressure $p=2.8$ Pa. For these conditions, we found a horizontal confinement potential of the form $Q\phi_{\mathrm{H}}(r)=b_{\mathrm{H}}r^2$, with $b_{\mathrm{H}}/Q=(0.50\pm 6\%)$ V/cm^2 and the distance from the center $r\lesssim 3$ mm. The particle charge was $Q=(15\,500\pm 5\%)e$ and the screening length $\lambda=(0.50\pm 10\%)$ mm. We also measured the resonance frequency of the vertical oscillations, which was $\Omega_{\mathrm{V}}/2\pi=(15.5\pm 1\%)$ Hz.

In the next step, we injected particles in groups of $\simeq 10$. The horizontal confining force pressed the particles together, so that a crystalline monolayer with a hexagonal structure formed in the center above the electrode. With increasing particle number, the interparticle distance decreased, with the smallest distance in the center (due to the ''parabolic'' radial confinement). Moving the laser sheet vertically, we determined after each injection that *no particles* were located above or below the crystalline monolayer. When the particle number exceeded a certain threshold, the monolayer started melting from the center to the periphery. For the experiment described here, the threshold number was $\simeq 170$, which corresponds to an interparticle distance $\simeq 0.55$ mm in the center. The horizontal particle trajectories during the melting process are shown in Fig. 1. Still, there were no particles located above or below the monolayer; however, the particles were oscillating in the vertical direction with amplitudes less than

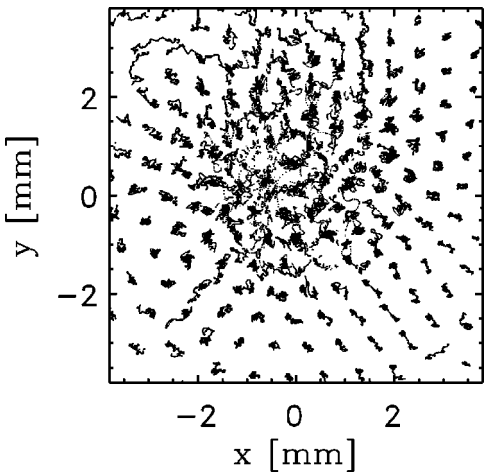

FIG. 1. Top view of the particle monolayer in the experiment (no particles levitating above or below). The particles are in crystalline state, until the density exceeds a certain threshold and the monolayer melts. The figure shows trajectories over 3.1 s after the melting starts.

$\simeq 20\%$ of the interparticle distance (technically, we could not record the side view with the video camera). The average kinetic energy of particles in the center saturated at ~ 30 eV.

Note that in every experiment, we were able to stop the melting by increasing the pressure (up to $\simeq 5-10$ Pa)—the system always returned to a stable crystalline monolayer. If the pressure was sufficiently high, the system never melted. In this case, when the number of the injected particles exceeded a certain threshold, the monolayer transformed into a bilayer system.

Simulation. We simulated these experimental phenomena using the dynamically shielded dust (DSD) particle simulation code [18]. The code contains a first-principles representation of the short-range shielded Coulomb forces and the wake forces due to the streaming ions. The effects of the ion-neutral collisions as well as neutral gas friction for the particles are included in the model.

The particles were loaded in a single horizontal plane. The vertical position of the plane was chosen such that the gravitational force on the particles balanced the force due to the sheath electric field. As in the experiment, the particles were confined in the horizontal direction by a weak radial electric field. By using the results of the single- and two-particle experimental studies described above, the magnitudes of the vertical and horizontal confining forces as well as the particle charge and plasma screening length were chosen to match the experimental values.

To begin the simulation runs, the particles were loaded at rest in concentric rings. The particles were then allowed to move under the combined mutual repulsive forces and the external forces. During each run, the number of particles and the pressure were held constant. A series of simulations was carried out with particle numbers and pressures chosen to span the parameters of the experiment. We used pressures of 2.8 (the experimental value), 5.6, and 7.0 Pa, and 100, 125, and 150 particles, respectively. At 2.8 Pa, the simulations with 100 and 125 particles were stable, while the simulation

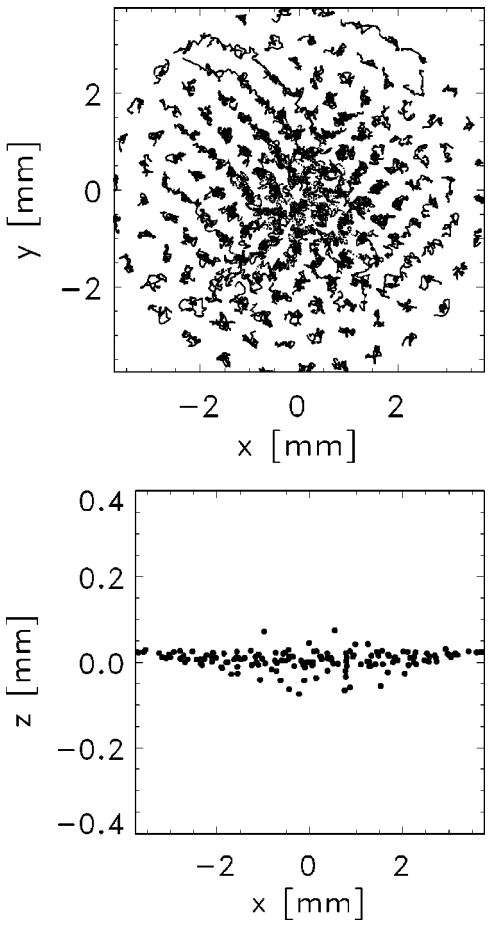

FIG. 2. (a) Top view of the particle monolayer in the DSD simulation with parameters similar to the experiment shown in Fig. 1. The figure shows trajectories over 3.1 s. As in the experiment, the instability occurs in the central region where the particle density is higher. (b) Side view of the monolayer. The simulation snapshot shows that the particles oscillate in the vertical direction as well as in the horizontal plane. In the experiment, the particles also oscillated vertically, but there was no diagnostic to record this motion.

with 150 particles was unstable. In the unstable case, the interparticle distance in the center was close to the experimentally measured value of $\simeq 0.55$ mm. The instability developed in a manner similar to the experiment: It started in the cental region of the system and expanded towards the periphery, with the particles oscillating in the horizonal and vertical directions (see Fig. 2). Note that the side view shown in Fig. 2(b) is also similar to that observed in the experiment. The saturated kinetic energy of the particles was $\simeq 20$ eV, which is about the experimental value. (The profile of the radial confinement in the experiment might deviate from the parabolic one at $r \gtrsim 3$ mm, becoming flatter. This could be the reason why the particle distribution at the periphery obtained in the simulation is somewhat different from that in the experiment.) In order to investigate the pressure dependence of the instability, we increased the pressure to 5.6 and 7.0 Pa for the 150 particle case. Although the simulation at 5.6 Pa appeared to be stable when viewing the particle motions, by monitoring the particle kinetic energy, we determined that at this pressure, the system was slightly unstable.

At 7.0 Pa, the particle kinetic energy completely decayed away, indicating that the system was in stable equilibrium.

Finally, we reexamined the case of the 2.8 Pa pressure used in the experiment. We reduced the particle interaction potential to a pure Yukawa potential (without wakes) in order to verify that the instability was induced by the particle-wake interaction. We ran simulations with 150, 200, and 250 particles and found that the system was always stable. For the case of 250 particles, a bilayer system was formed in the central region, with layers above and below the injection plane.

Theory. There exist three types of DL waves in a crystalline monolayer: longitudinal (acoustic), transverse (acoustic), and transverse (optical) modes. The longitudinal mode is a compressional wave, while the transverse acoustic mode is a shear wave. Both are due to horizontal (in-plane) motion of particles [19]. The transverse optical mode is associated with vertical (out-of-plane) oscillations [15,20]. Theoretical analysis of the DL modes becomes simplified when the so-called ''1D string model'' is used [20,21]. The long-wavelength dispersion relations obtained for 2D lattices [19] have been shown to be nearly coincident with those for 1D strings [22].

Recently, Ivlev and Morfill [15] have studied theoretically the influence of wakes on the longitudinal and transverse (optical) DL modes in a monolayer. We briefly summarize these results: Negatively charged particles of charge $-Q$ and mass M are separated horizontally by a distance Δ and interact via a screened Coulomb (Yukawa) potential with screening length λ. The lattice parameter $\kappa=\Delta/\lambda$ usually exceeds unity [5,23], and therefore, only the nearest neighbor interactions are taken into account. The excess positive charge of the wake, q, is approximated by a pointlike charge located at distance δ downstream from the particle. Vertically, the particles are confined in a potential well with the resonance frequency Ω_{V}. It was shown that the longitudinal ($\parallel$) and the transverse ($\perp$) modes are coupled due to the particle-wake interaction [15]. When the coupling is weak, the dispersion relations for the branches are

$$\mathrm{Re}\ \ \omega_{\parallel}\simeq 2\Omega_{\parallel}\sin\left(\frac{1}{2}k\Delta\right),$$

$$\mathrm{Re}\ \ \omega_{\perp}\simeq\sqrt{\Omega_{\mathrm{V}}^2-4\Omega_{\perp}^2\sin^2\left(\frac{1}{2}k\Delta\right)}. \qquad (1)$$

Here $\Omega_{\parallel}^2\simeq(1-\tilde{q})(2+2\kappa+\kappa^2)\Omega_0^2$ and $\Omega_{\perp}^2\simeq(1-\tilde{q})(1+\kappa)\Omega_0^2$ are the frequency scales for the modes, with $\Omega_0^2=(Q^2/M\Delta^3)e^{-\kappa}$ and $\tilde{q}=q/Q$. The wave number k is within the first Brillouin zone: $|k|\Delta\leqslant\pi$. The branches of Eq. (1) are assumed to be weakly damped, with the damping rate γ due to neutral gas friction: $\mathrm{Im}\ \omega_{\parallel}\simeq\mathrm{Im}\ \omega_{\perp}\simeq\gamma$ (note that the damping rate is proportional to the gas pressure). In the absence of wakes ($\tilde{q}=0$), Eq. (1) reduces to the results obtained in Ref. [20].

Coupling of DL modes becomes strong when branches (1) intersect, as shown in Fig. 3. The condition for that is $4(\Omega_{\parallel}^2+\Omega_{\perp}^2)>\Omega_{\mathrm{V}}^2$ [15] or

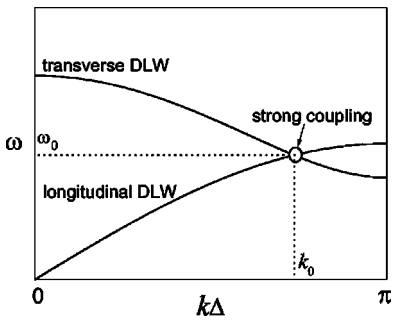

FIG. 3. Longitudinal (acoustic) and transverse (optical) branches of the dust-lattice waves (DLW). When the branches intersect, the particle-wake coupling can drive an instability in the vicinity of (ω_0,k_0).

$$\eta\equiv 4(1-\tilde{q})(3+3\kappa+\kappa^2)\left(\frac{\Omega_0}{\Omega_{\mathrm{V}}}\right)^2>1 \qquad (2)$$

The value of Ω_0^2 rapidly increases with the particle density (i.e., as Δ decreases). Hence, there is a critical value of the density above which the coupling between the branches is strong. The point where the branches intersect, (ω_0,k_0), is given by the following expressions: $\omega_0=\sqrt{(2+2\kappa+\kappa^2)/(3+3\kappa+\kappa^2)}\Omega_{\mathrm{V}}$ and $\sin(\frac{1}{2}k_0\Delta)=\frac{1}{2}\omega_0/\Omega_{\parallel}$. The strength of the coupling is determined by the frequency scale $\Omega_{\mathrm{coup}}^2\simeq\tilde{q}\tilde{\delta}(3+3\kappa+\kappa^2)\Omega_0^2$, with $\tilde{\delta}=\delta/\Delta$. The branches are modified and form a hybrid branch in a narrowvicinity around the intersection point, $|k-k_0|/k_0\sim(\Omega_{\mathrm{coup}}/\omega_0)^2$, where the resonance coupling *drives an instability* with $\mathrm{Im}\ \omega\simeq\gamma-(\Omega_{\mathrm{coup}}^2/\omega_0)\sin(k_0\Delta)$. The energy source for the instability is provided by the ion flux through the interaction of particles with the wakes. If the pressure is sufficiently low, the neutral gas damping γ does not suppress the instability. We get the following threshold value for the damping [using the definition of Ω_{coup}, ω_0, and k_0, as well as condition (2)]:

$$\frac{\gamma}{\Omega_{\mathrm{V}}}<\frac{\tilde{q}\tilde{\delta}}{2(1-\tilde{q})}\sqrt{\frac{3+3\kappa+\kappa^2}{2+2\kappa+\kappa^2}}\sqrt{\eta-1}. \qquad (3)$$

Thus, Eqs. (2) and (3) are the conditions for the coupling instability: Inequality (2) determines the particle density threshold which is necessary for the instability onset, and inequality (3) gives the pressure threshold below which the instability can be driven. If the gas pressure is high enough, the particles remain stable as the density increases, until the so-called ''zig-zag'' transition occurs (see, e.g., Ref. [24])—particles are pushed out of the plane due to mutual repulsion. In accordance with Eq. (1), the transition starts when $2\Omega_{\perp}>\Omega_{\mathrm{V}}$. Note that the density threshold for this transition is higher than that for the instability onset [Eq. (2)], i.e., when the density increases the instability (unless suppressed) always starts first. All these features are observed in the experiments and simulations: As we increase the particle density, a monolayer melts once the density exceeds a threshold. This phenomenon occurs at sufficiently low pressures. If the

pressure is high enough, the melting does not start but instead the monolayer transforms into two layers (which corresponds to the zig-zag transition). Substituting parameters measured in the experiment ($Q \simeq 15\,500e$, $\lambda \simeq 0.5$ mm, $\Omega_V/2\pi \simeq 15.5$ Hz) and derived from the simulation ($\tilde{q} \simeq 0.5$) into the density threshold condition [Eq. (2)], we get the critical value of the particle separation of $\Delta \simeq 0.5$ mm. This is very close to the experimentally (and numerically) obtained threshold. The pressure sufficient to suppress the instability is $p \simeq 6$ Pa, as derived from Eq. (3) (we took $\tilde{\delta} \simeq 0.5$ obtained from the simulations). This is also in very good agreement with the numerically obtained threshold $5.6 < p < 7.0$ Pa.

In conclusion, we studied melting of the monolayer plasma crystals in a rf discharge. We compared the experimental results with molecular dynamics simulations and theory and showed that the melting is induced by the resonance coupling of the dust-lattice wave modes due to interaction of particles with plasma wakes. The instability that causes the melting starts when the particle density in the monolayer exceeds a certain threshold. The melting occurs when the gas pressure is sufficiently low, otherwise the monolayer remains stable until it transforms into a bilayer system.

G.J. was supported in part by NASA. A.V.I. and U.K. were supported by DLR under Contract No. 50 WP 0203.

[1] H. Thomas *et al.*, Phys. Rev. Lett. **73**, 652 (1994).
[2] J.H. Chu and L. I, Phys. Rev. Lett. **72**, 4009 (1994).
[3] J.B. Pieper, J. Goree, and R.A. Quinn, Phys. Rev. E **54**, 5636 (1996).
[4] Y. Hayashi, Phys. Rev. Lett. **83**, 4764 (1999).
[5] M. Zuzic *et al.*, Phys. Rev. Lett. **85**, 4064 (2000).
[6] H.M. Thomas and G. Morfill, Nature (London) **379**, 806 (1996).
[7] J.B. Pieper, J. Goree, and R.A. Quinn, J. Vac. Sci. Technol. A **14**, 519 (1996).
[8] G.E. Morfill *et al.*, Phys. Plasmas **6**, 1769 (1999).
[9] H. Schollmeyer, A. Melzer, A. Homann, and A. Piel, Phys. Plasmas **6**, 2693 (1999).
[10] V.A. Schweigert *et al.*, Phys. Rev. E **54**, 4155 (1996).
[11] G. Joyce, M. Lampe, and G. Ganguli, Phys. Rev. Lett. **88**, 095006 (2002).
[12] F. Melandso and J. Goree, Phys. Rev. E **52**, 5312 (1995).
[13] S.V. Vladimirov and M. Nambu, Phys. Rev. E **52**, R2172 (1995).
[14] I.V. Schweigert *et al.*, Phys. Rev. E **62**, 1238 (2000).
[15] A.V. Ivlev and G. Morfill, Phys. Rev. E **63**, 016409 (2000).
[16] P.J. Hargis, Jr. *et al.*, Rev. Sci. Instrum. **65**, 140 (1994).
[17] U. Konopka, G.E. Morfill, and L. Ratke, Phys. Rev. Lett. **84**, 891 (2000).
[18] G. Joyce, M. Lampe, and G. Ganguli, IEEE Trans. Plasma Sci. **29**, 238 (2001).
[19] F.M. Peeters and X. Wu, Phys. Rev. A **35**, 3109 (1987).
[20] S.V. Vladimirov, P.V. Shevchenko, and N.F. Cramer, Phys. Rev. E **56**, R74 (1997).
[21] F. Melandsø, Phys. Plasmas **3**, 3890 (1996).
[22] D. Samsonov, Ph.D. thesis, The University of Iowa, 1999.
[23] A.P. Nefedov *et al.*, New J. Phys. **5**, 33 (2003).
[24] D.H.E. Dubin and T.M. O'Neil, Rev. Mod. Phys. **71**, 87 (1999).